The 20th International Flow Measurement Conference FLOMEKO 2026

# Ultra-low-speed anemometer calibrations in a bench-top wind tunnel

**C J Crowley[1*], J N Kumar[1], I I Shinder[1]**

[1] National Institute of Standards and Technology, 100 Bureau Drive, Gaithersburg, Maryland 20899, USA
* E-mail: christopher.j.crowley@nist.gov

## Abstract

Accurate calibration of anemometers at ultra-low airspeeds (i.e. speeds below 1 m/s) is essential for applications such as indoor airflow measurement, cleanroom monitoring, and environmental sensing. To address this need, the National Institute of Standards and Technology has modified a bench-top wind tunnel to produce stable flows in the range of less than 0.1 m/s to 5 m/s and to support optical and image-based measurement techniques. The test section of the tunnel measures approximately 15 cm × 15 cm, and typical anemometers may occupy up to 5 % of this cross-sectional area. While a compact wind tunnel offers advantages in achieving and controlling low-speed flows, it also presents unique challenges. Chief among these are the blockage effects introduced by the sensor itself and the influence of nearby tunnel walls, both of which can significantly distort the local flow field and reduce calibration accuracy. This work discusses mitigation strategies including blockage correction methods and tunnel design considerations. Numerical simulations indicate that the effects of both sensor and wall blockage can be quantified and largely corrected. Preliminary experimental results support the simulation findings, though further refinements to the tunnel design are needed to fully validate and implement the corrections.

## 1. Introduction

Accurate measurement of airflow at airspeeds below 1 m/s is essential for applications such as indoor airflow measurement, cleanroom monitoring, and environmental sensing. To provide SI-traceable measurements in these applications, anemometers must be calibrated at or below the airspeeds at which they are used. Currently only five national metrology labs provide SI traceable calibrations down to 0.1 m/s with their uncertainties near 10 % [1] and inter-comparison studies demonstrate how difficult these calibrations are. [2] Because anemometers vary widely in size, shape, and operating principle, the only universal calibration approach is to install them in a wind tunnel and compare their readings to SI-traceable measurements of the free-stream airspeed to which the anemometer is exposed.

The goal of an anemometer calibration is to produce a calibration factor

$$v_\infty = C v_{\mathrm{IUT}} \tag{1}$$

which relates the reading of the instrument under test, $v_{\mathrm{IUT}}$, to the true airspeed of an infinitely large, uniform flow moving at $v_\infty$. In practice, accurately determining $C$ in a wind tunnel requires careful consideration of all ways in which the flow in the tunnel is not a stable, infinitely large, uniform flow. One of the most important effects is the blockage effect [3, 4, 5] caused by the instrument itself disturbing the flow. As the required calibration airspeed decreases, several other challenges arise, chief among them the generation of stable airflow.

Generating airflow at speeds below approximately 1 m/s in a large wind tunnel, such as the primary wind tunnel at the National Institute of Standards and Technology (NIST), is challenging for several reasons. NIST's primary wind tunnel is a closed-loop facility with a test-section cross-section of 1.5 m × 2. m. [6] The large physical size of the tunnel implies a correspondingly large mass of air that must be accelerated and precisely controlled, placing stringent demands on the control system. Achieving such low airspeeds also requires the fan to operate at very low rotational speeds, where its efficiency is significantly reduced. Together, these factors make it difficult to produce and maintain stable, low-speed flow.

To overcome these challenges, NIST has modified a bench-top wind tunnel to produce stable flows in the range from below 0.1 m/s to 5 m/s, enabling the calibration of ultra-low-speed anemometers. The bench-top tunnel is an Eiffel-type (*i.e.*, open-loop) tunnel with a test section

approximately 15 cm × 15 cm in cross-section and 50 cm in length. The smaller scale of the tunnel allows the fan and control system to operate at substantially lower power, alleviating challenges associated with high-power control at low speeds. To further mitigate issues associated with low fan rotational speeds, a pressure-drop element can be installed downstream of the test section. This additional pressure drop allows the fan to operate at higher, more efficient rotational speeds, thereby enabling stable, low-power control of the airflow.

However, the use of a smaller wind tunnel introduces new challenges. The significantly reduced test-section cross-section means that a typical anemometer occupies a non-negligible fraction of the flow area, making blockage effects significant. For example, a typical Pitot tube with an 8 mm diameter has a projected cross-sectional area equal to approximately 3.4 % of the test-section area. The presence of the anemometer therefore alters the flow field within the tunnel, complicating the inference of the appropriate free-stream airspeed to ascribe to the instrument. In this paper, we describe a procedure for quantifying and correcting for blockage effects in ultra-low-speed wind-tunnel calibrations based on numerical studies.

Section 2 of this paper outlines the conceptual framework, Section 3 describes the numerical setup, Section 4 presents the results, and then in Section 5 is a discussion of the take-away of this study.

## 2. Conceptual Approach to Quantifying Blockage Effects

The presence of an anemometer within a confined wind-tunnel test section introduces a coupled fluid–structure interaction in which the instrument and the surrounding flow influence one another. In general, introducing a probe may alter the pressure and velocity distributions throughout the entire test section, such that the resulting flow cannot be interpreted as a simple perturbation of an underlying "undisturbed" state. Under these conditions, the free-stream velocity that would exist in the absence of the probe is no longer directly accessible or relevant, and the interpretation of calibration measurements becomes nontrivial; there is no direct way to measure the "true" flow experienced by the instrument. In the most general case, resolving this ambiguity would require a geometry-specific analysis accounting for both the probe and the wind-tunnel configuration.

When the characteristic size of the probe is small relative to the test-section cross-sectional area, however, the resulting flow disturbance may remain spatially confined. In such cases, the probe-induced modification does not fundamentally reshape the global tunnel flow, and the dominant effects are largely limited to the vicinity of the probe and its downstream wake. The validity of this approximation depends on probe geometry, blockage area ratio, and location within the flow.

In the present work, this issue is addressed by numerically examining the spatial extent of the flow modification caused by a Pitot tube installed in a small, bench-top wind tunnel. The numerical domain and inlet conditions are chosen such that it represents those of the bench-top wind tunnel NIST has recently acquired and modified. The study is designed to determine whether the probe-induced disturbance remains localized or pervades the test section.

The analysis proceeds by first characterizing the flow without any probe, establishing a reference state of the tunnel's velocity and pressure fields absent an instrument. The Pitot tube is then introduced at several axial locations, and the resulting flow fields are compared directly to the empty-tunnel case. Both the empty and probe-occupied configurations are adjusted to have the same velocity at a reference point, mimicking the experimental procedure in which a non-intrusive measurement, such as a laser Doppler anemometer (LDA), is used to set the flow and provide the SI traceable measurement of the free-stream speed. This approach provides a quantitative basis for assessing the magnitude and spatial extent of probe-induced flow modifications.

For the configuration considered here, the numerical results indicate that the dominant effects of the Pitot tube are confined to the region near the probe and its downstream wake, while the broader flow remains largely unaffected. This observation motivates interpreting the flow non-uniformity experienced by the probe as the combined effect of intrinsic tunnel gradients and localized distortions introduced by the instrument.

## 3. Numerical setup

Numerical simulations were performed using a RANS model in COMSOL Multiphysics 6.3 [7] to model the wind tunnel described in Section 1. Two configurations were considered: an empty test section and a test section containing a standard, 8 mm diameter Pitot tube (Sensing Precision L-Type Pitot Probe). The dimensions of the Pitot tube were made to match the specific geometry of a Pitot tube that NIST had on hand. The computational domain represents the full tunnel flow path, including regions upstream of the test section and mesh refinement was performed near the wind tunnel intake to preserve system-level pressure–flow behavior.

For the probe-installed configuration, the Pitot tube was positioned along the tunnel centerline at several axial locations parameterized by the non-dimensional distance $L/D$, where $L$ is the axial distance from the measurement location (*e.g.* the LDA's location) and $D$ is the probe diameter. The range of $L/D$ values was limited by the physical geometry of the test section.

Simulations were conducted at nominal freestream veloc-

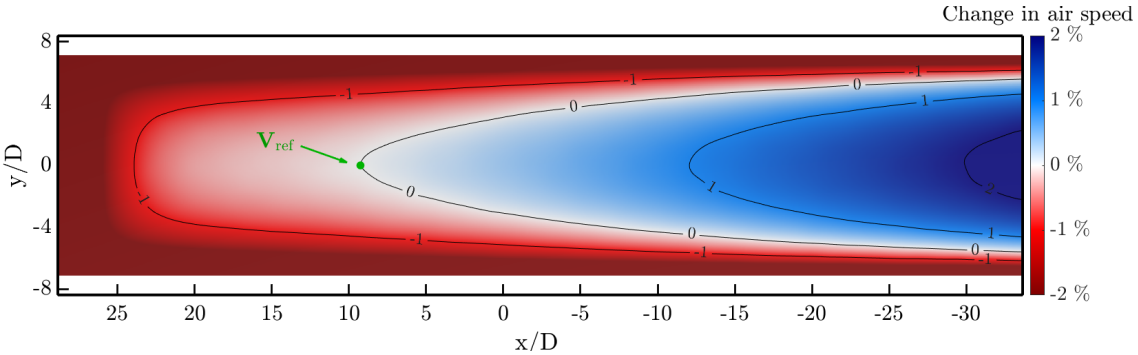


**Figure 1:** Center plane airspeed field of the empty wind tunnel test-section computed numerically. Flow moves from the left to the right at 5 m/s. The color map represent percentage deviation in the air speed compared to the airspeed at the reference location marked with the green dot. Note that there is gradient in the airspeed in all three dimensions, which are as large as $\pm 1\%$.

ities of 1 m/s, 3 m/s, 5 m/s, 7 m/s, and 10 m/s. Rather than prescribing an inlet velocity, the outlet pressure was adjusted such that a specified axial velocity was achieved at a reference point corresponding to the LDA measurement location in our actual tunnel. This velocity constraint was applied consistently to both the empty-tunnel and probe-installed cases, mimicking the experimental procedure in which the tunnel speed is set using a non-intrusive reference measurement. A velocity goal-seeking procedure was employed to determine the outlet pressure required to achieve the target reference velocity. For each nominal velocity, goal-seeking was performed for the empty tunnel and for the probe-installed case at the largest $L/D$ to compute the tunnels total blockage-based pressure drop, which was assumed to not depend on the axial location of the probe. The resulting outlet pressure was then held fixed for all remaining probe locations at the same velocity, allowing probe-induced flow modifications to be compared under consistent operating conditions.

The computational mesh was refined locally in the vicinity of the Pitot tube and its downstream wake to resolve probe-induced gradients, while coarser resolution was used elsewhere to maintain computational efficiency. Final meshes contained approximately $5 \times 10^5$ vertices and were found to adequately resolve the flow features of interest.

Velocity and pressure fields were exported for post-processing. For the probe-installed cases, static and stagnation pressures were evaluated at locations corresponding to the physical Pitot tube ports and used to assess probe-induced flow modifications as a function of axial position and freestream velocity.

## 4. Results

Figure 1 shows the numerically computed center-plane airspeed field for the empty wind-tunnel test section. The color map represents the percentage deviation of the local airspeed relative to the airspeed at the reference location, indicated by the green marker. Even in the absence of any probe, the flow is not spatially uniform: gradients in airspeed are present in all three spatial directions, with deviations of up to approximately $\pm 1$ % relative to the reference value. These gradients arise primarily from a growing boundary layer in the tunnel along the tunnel axial direction and mass flow conservation. As a result, an anemometer placed at a location $(x/D, y/D, z/D)$ will, in general, experience a different airspeed than that measured by a non-intrusive LDA system located at the reference point.

The presence of these spatial gradients mean that a direct comparison of the reference LDA and an anemometer placed somewhere else within the test section would not constitute a calibration since the anemometer would experience a different “free-stream” airspeed just due to its different location in the gradient. Figure 2 shows the corresponding center-plane airspeed field when a Pitot tube is installed along the tunnel centerline, operated at the same nominal flow setpoint as in Figure 1. In this case, the colormap represents the percentage deviation of the local airspeed relative to the empty-tunnel reference field. The presence of the Pitot tube produces a localized disturbance in the flow field, characterized by a region of accelerated flow around the probe and a downstream wake. Importantly, sufficiently far upstream of the Pitot tube, the deviation from the empty-tunnel flow field is negligible. This indicates that, for the configuration considered here, the probe-induced blockage effect does not pervade the entire test section but remains spatially confined.

This result has direct implications for the calibration procedure. Provided that the reference measurement location is sufficiently far (this study found $L/D$ approximately 10 or greater) upstream of the Pitot tube, the influence of the probe on the flow at the LDA location is 0.001 %, which is negligible compared to other uncertainty factors. Under these conditions, the free-stream airspeed measured by the LDA remains a valid, SI-traceable reference for setting the tunnel operating condition during calibration.

However, as demonstrated in Figure 1, the intrinsic ve-

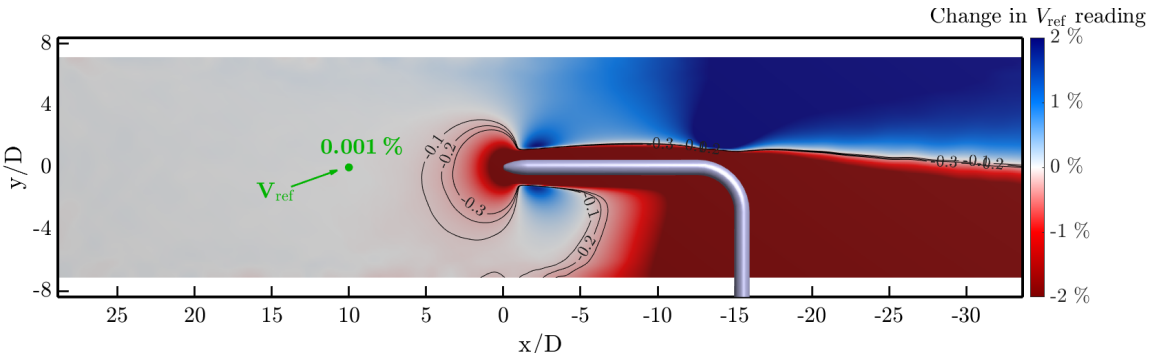


**Figure 2:** Numerically computed center plane airspeed field of the wind tunnel with the Pitot tube installed in the center of the test-section. Flow moves from the left to the right at 5 m/s. The color map represent percentage deviation in the air speed compared to the airspeed reference field. Note that the deviation from the empty tunnel field sufficiently far upstream of the Pitot tube is negligible, meaning the effect is localized.

locity gradients present in the empty tunnel imply that the airspeed measured at the LDA reference location cannot, in general, be directly assigned to the Pitot tube measurement location. Even in the absence of probe-induced blockage, spatial variations in the flow lead to systematic differences between the local airspeed experienced at the instruments location and the reference measurements location. To account for this effect, the empty-tunnel flow field is characterized to determine a position-dependent correction factor that relates the local airspeed at the probe location to the reference airspeed measured by the LDA. This correction factor, often called the "position correction", is a function of spatial location $(x, y, z)$ and nominal airspeed as measured at the position of the reference LDA $(x_{\text{ref}})$

$$C_{\text{pos.}}\left(x, y, z, v_{\text{ref}}\right) = \frac{v_x\left(x, y, z\right)}{v_x\left(x_{\text{ref}}, y_{\text{ref}}, z_{\text{ref}}\right)} \qquad (2)$$

Example centerline correction factors derived from the numerical simulations are shown in Figure 3.

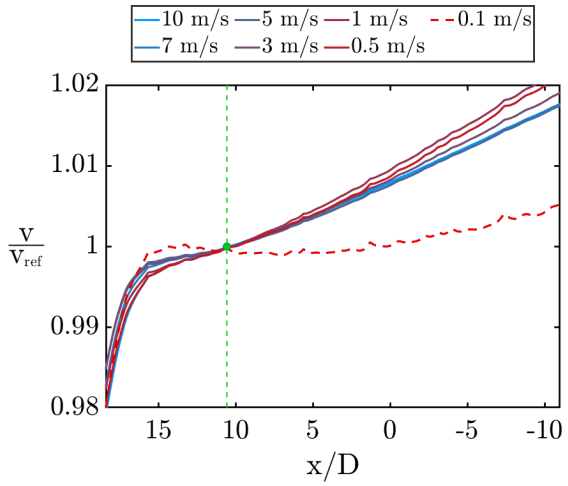


**Figure 3:** Centerline position correction factors as a function of $x/D$. This airspeed dependent correction function accounts for the natural gradient that is present in the test section absent an anemometer.

In addition to the position correction made in Equation 2, the gradients formed by the growing boundary layer in the tunnel may also affect how the instrument itself performs, thereby affecting the calibration. This is the case, for example, with a Pitot tube. A Pitot tube subtracts the measured static pressure from the measured total pressure to infer the flow pressure, but the static pressure measured on the downstream surface ports of the tube are not the same static pressure as the port on the tip of the probe. In the analysis here this effect has been neglected; however, this effect may be important and needs to be investigated.

## 5. Discussion

The numerical results demonstrate that two distinct effects must be addressed when performing ultra-low-speed anemometer calibrations in a small wind tunnel: intrinsic spatial gradients in the tunnel flow from the confined test section and probe-induced blockage effects. Even in the absence of an anemometer, wall friction and flow development produce measurable, non-negligible, velocity gradients throughout the test section, with magnitudes on the order of $\pm 1\%$ in our test section. The spatial gradient in velocity has a few effects in the calibration (*e.g.*, position dependence of IUT, the IUT's reading is affected by the gradient, and *etc.*), but typically the largest effect is the position dependence. These gradients imply that a reference airspeed measured at a single location cannot, by itself, be assumed to represent the airspeed experienced by an instrument placed elsewhere in the flow.

The simulations further show that, for the Pitot tube geometry and operating conditions considered here, the blockage effect introduced by the probe remains spatially localized. Beyond a sufficiently large upstream separation from the reference measurement – approximately $L/D \gtrsim 10$ in this study – the probe has a negligible influence on the flow at the reference measurement location. This observation supports a calibration strategy in which a non-intrusive reference measurement, such as LDA, may be used to establish the tunnel operating condition without being contaminated by the presence of the instrument un-

der test.

Importantly, the localization of the blockage effect is not assumed *a priori* but emerges from the numerical analysis. In the most general case, the introduction of a probe could alter the global flow field in a non-separable manner, rendering the concept of an "empty-tunnel" reference meaningless. The present results indicate that such global flow disturbance does not occur for the probe size, blockage ratio, and flow regime examined here. However, this conclusion should not be generalized without caution. The degree to which blockage effects remain localized will depend on probe geometry, frontal area, placement within the test section, and tunnel dimensions. Establishing quantitative criteria for when this approximation breaks down remains an important topic for future investigation.

If the blockage effect is non-local or cannot be mitigated due to tunnel-specific constraints, probe-geometry-specific corrections is required. This blockage correction can be determined experimentally when calibrating multiple instruments of the same type in the same location of the tunnel. In that case, a representative instrument can be calibrated in a larger wind tunnel and then recalibrated in the smaller tunnel. The difference between these calibrations provides the blockage correction for an instrument of that size and shape at that location. This correction can then be applied to subsequent calibrations of similar instruments installed in the same position. If this approach is not feasible, additional investigation is required to determine an appropriate blockage correction factor.

When the blockage effect is localized, calibration accuracy is instead limited by the intrinsic flow gradients of the tunnel. In this regime, the appropriate free-stream airspeed to assign to the instrument is not the reference airspeed itself, but the reference airspeed corrected to the instrument location using a position-dependent correction factor

$$C = C_{\text{pos.}} \frac{v_{\text{ref}}}{v_{\text{IUT}}} \tag{3}$$

where $v_{\text{IUT}}$ is the airspeed indicated by the instrument under test. It should be noted that Equation 3 implicitly assumes that $v_{\text{ref}} = v_{\infty}$, which is only approximately true (*e.g.*, the anemometer itself may be affected by the flow gradients), and in general, needs to be further corrected. The results demonstrate that such correction factors can be determined from a characterization of the empty-tunnel flow field and applied consistently across operating conditions.

Although the position correction functions presented here are derived from numerical simulations, their role in an SI-traceable calibration requires experimental determination. In practice, this characterization must be performed using non-intrusive measurement techniques, such as LDA or Particle Image Velocimetry (PIV), to map the velocity field throughout the empty test section. Once established, these correction factors can be applied to subsequent calibrations, provided the tunnel configuration remains unchanged.

Overall, the results support a calibration framework in which (i) the reference measurement is placed sufficiently far upstream to avoid probe-induced disturbance, and (ii) intrinsic tunnel gradients are accounted for through a prior characterization of the empty flow. This approach enables accurate, SI-traceable calibrations of small anemometers in compact, ultra-low-speed wind tunnels, while clearly delineating the assumptions under which it remains valid.

## References


[1] Bureau International des Poids et Mesures (BIPM). Key comparison database (kcdb): Calibration and measurement capabilities (cmcs). https://www.bipm.org/kcdb. accessed November 2025.

[2] D. Pachinger, M. de Huu, H. Mueller, I. Care, E. Birt, et al. Euramet project no. 1225: intercomparison of very low air speed standard facilities (0.05 m/s to 1 m/s). *Metrologia*, 54(1A):07021, 2017.

[3] Wu Jian and Chua Hock Ann. Blockage Effects in the Calibration of Anemometer in a Wind Tunnel. Taipei, Taiwan, October 2010.

[4] J Geršl, P Busche, M de Huu, D Pachinger, H Müller, K Hölper, A Bertašienė, M Vilbaste, I Care, H Kaykısızlı, L Maar, and S Haack. Comparison of calibrations of wind speed meters with a large blockage effect. June 2019.

[5] G. Bobovnik, P. Sambol, J. Geršl, and J. Kutin. Experimental investigation of a vane probe blockage effect in a small wind tunnel. *Measurement*, 261:119919, February 2026.

[6] Iosif I. Shinder, Christopher J. Crowley, B. James Filla, and Michael R. Moldover. Improvements to NISTS air speed calibration service. *Flow Measurement and Instrumentation*, 44:19–26, August 2015.

[7] COMSOL AB. *COMSOL Multiphysics® v6.3*. COMSOL AB, Stockholm, Sweden, 2024. Finite element analysis software.